Mathematical Models of Hepatitis B Virus Dynamics during Antiviral Therapy

Andrea Carracedo Rodriguez

Thesis submitted to the Faculty of the
Virginia Polytechnic Institute and State University
in partial fulfillment of the requirements for the degree of

Master of Science
in
Mathematics

Stanca M. Ciupe, Chair
Matthias Chung
John F. Rossi

March 25, 2016
Blacksburg, Virginia

Keywords: Mathematical modeling, Hepatitis B treatment, Viral decay profiles

Mathematical Models of Hepatitis B Virus Dynamics during Antiviral Therapy

Andrea Carracedo Rodriguez

(ABSTRACT)

Antiviral therapy for patients infected with hepatitis B virus is only partially efficient. The field is in high demand for understanding the connections between the virus, immune responses, short-term and long-term drug efficacy and the overall health of the liver. A mathematical model was introduced in 2009 to help elucidate the host-virus dynamics after the start of therapy. The model allows the study of complicated viral patterns observed in HBV patients. In our research, we will analyze this model to determine the biological markers (e.g. liver proliferation, immune responses, and drug efficacy) that determine the different decay patterns. We will also investigate how such markers affect the length of therapy and the amount of liver damage.

Contents

List of Figures

List of Tables

Chapter 1

Introduction

Antiviral therapy for patients infected with hepatitis B virus is only partially efficient. The field is in high demand for understanding the connections between the virus, immune responses, short-term and long-term drug efficacy and the overall health of the liver. Mathematical models can help elucidate the host-virus dynamics after start of therapy. Such a model was introduced in 2009 by Dahari *et al.* to study the complicated viral patterns observed after the start of therapy. They range from biphasic, triphasic, flat phase, to virus rebound. In this thesis we use analytical and numerical techniques that provide connections between the observed patterns, virus and host characteristics, drug efficacy and liver health. The thesis is structured as follows: In chapter 2, we introduce biological background for the hepatitis B virus, its outcomes and the available human intervention. In chapter 3, we present background for the mathematical models of hepatitis B virus deveoped in the last 20 years, culminating with the Dahari model that is used in the thesis. In chapter 4 we give an introduction to the numerical analysis methods that we will use to obtain information about the model. In chapters 5 and 6 we present analytical and numerical results found from analyzing the model. In chapter 7 we discuss our results and propose future directions.

Chapter 2

Biological background

2.1 Hepatitis B infection

Hepatitis B is a dangerous liver disease spread all around the world with high rates of infection in underdeveloped countries. About 350 million people have chronic HBV, up to 2 million die every year, making it the 9th leading cause of death. As much as 30% of the world's population was at some point infected with HBV [36]. The disease is caused by the hepatitis B virus (HBV) which is transmitted through contact with the body fluids of an infected person, during unprotected sexual relationships, and from an infected mother to infant during delivery. Some of the improvements made towards prevention of hepatitis B infection are testing blood donors and vaccinating newborns (we will give more details about vaccination later in this chapter) [23, 31]. There have also been campaigns to make people aware of the danger of this disease [23].

Infection with HBV can lead to either acute or chronic infections but the reason behind these different outcomes is not known [50]. Most patients with chronic HBV are infected during or soon after birth [50]. According with WHO, more than 90% of infected adults will recover naturally within the first year of infection, and some of them will not even show symptoms of the disease [23]. This is a dangerous aspect of hepatitis B infection since a person could be infected but not be aware of it and, therefore, at a higher risk of transmitting the virus.

Hepatitis B infection leads to high virus production, up to 10^{10} copies per mL that last several weeks during acute infection [43]. During this time, up to 90% of liver cells, hepatocytes, gets infected [6, 33, 34, 45]. Liver damage is produced when the immune response kills the infected hepatocytes [23]. Progress understanding such immune response has been made studying the behavior of infected chimpanzees, woodchucks, ducks, and transgenic mice [43]. In particular, woodchucks with chronic infection develop hepatocellular carcinoma (HCC) and liver cirrhosis similarly to humans which makes them useful for clinical trials [20].

Experiments with woodchucks have shown that clearance of the virus can occur rapidly even if most hepatocytes are infected [34, 19]. To explain this fact, Guo *et al.* [50] designed a molecular study to identify the mechanisms that regulate virus clearance from infected hepatocytes. Their results show that recovery is due to a high increase in the number of CD8 T cells (which are the lymphocytes responsible for the cell-mediated immune system responses). CD8 T cell elevation is correlated with the expression of cytokines (cell signaling proteins) and killing of infected hepatocytes [50]. This has led to the conclusion that CD8 T cell mediated immune response plays an important role during infection, being responsible for both pathogenesis, and clearance. While it is accepted that hepatocyte death is CD8 T cell mediated, the non-cytolitic roles of CD8 T cells are still under investigation. It is believed that lymphocytes produce cytokines that cure infected cells and that newly regenerated hepatocytes not only loose the virus but become immune to reinfection [50, 43].

It is well known that the liver has the ability to self-regenerate [17, 48, 18]. A patient who overcomes acute HBV infection will restore their liver completely by mitotic division of hepatocytes [48]. In patients with high liver loss due to chronic infection, a reserve population of progenitor cells is activated (in addition to division of hepatocytes) to help liver regenerate faster [13].

There is no specific treatment for patients with acute infections. As mentioned above, most of these patients do not show any symptoms. For the ones who do suffer symptoms, such as extreme fatigue, nausea, vomiting and abdominal pain, the treatment would include the recovery of nutrients. Note that, although acute infection seems "easy" to overcome, there are some few cases in which the liver of the patient fails causing death [29].

For chronic patients, there are several options for therapy but none of them is 100% efficient. A summary is presented later in this chapter.

In this thesis, we will focus on the study of the dynamics of hepatitis B virus in patients chronically infected and receiving drug therapy at the time of the study. These patients are at high risk of developing liver cirrhosis or hepatocellular carcinoma (between 20% and 30% cases [23]).

2.2 Vaccination

Since 1982 a vaccine against HBV infection has been available [49]. Today the group that vaccination focuses on is the one with highest risk of developing chronic infection: children less than 6 years old [23]. According to Trepo *et al.* [31], 40% of men and 15% of women with HBV infection acquired at birth die of liver cirrhosis or hepatocellular carcinoma. The optimal vaccination strategy is for newborns to receive the first dose within the first 24h after birth and two boosters during their childhood. In 95% of the cases, the children will be protected from infection for at least 20 years, and they may be immune for life [23]. As a consequence, the number of liver cancer cases has diminished [36].

To reduce the number of HBV infections even more, it is recommended to vaccinate other high risk groups such as patients who require transplantations or dialysis, health-care workers, travelers before visiting an endemic area, people in prisons, or people with multiple sexual partners. [23]

The vaccine gives positive predictions about the eradication of the disease. However, it will take some years before vaccination is available to everyone. This is why we need a good therapy to cure patients that are already infected and have progressed to chronic disease.

2.3 Treatment of chronic HBV infection

Chronic hepatitis B has been proven to be a difficult disease to overcome needing long therapies in many cases. In general, for any viral infection, a long therapy could loose effectiveness with time since the virus may develop resistance to the drugs. When a patient is diagnosed with chronic HBV infection, if the patient is in the early stages of the disease and the level of antigens is low, it may be better to wait until the virus replication and damage of the liver is high. However, the decision depends on each patient's personal situation and predisposition to other diseases such as cirrhosis or HCC. [30]

There are currently seven approved drugs for the treatment of hepatitis B: two formulations of interferon (IFN): conventional and pegylated IFN (PEG-IFN), and five nucleos(t)ide analogues: lamivudine (LMV), telbivudine, adefovir, entecavir, and tenofovir [30]. Treatment with a nucleos(t)ide is potent, it inhibits virus replication in most patients for at least 5 years [8]. However, it is not possible to predict how long the treatment will take (some treatments are 5 years long) [8]. Also, all the nucleos(t)ide analogues are known to induce drug resistance so, in most cases, treatment is delayed or stopped which frequently results in a virus relapse [8]. Treatment using interferon is the most recommended [30] but it has some downsides compared to tenofovir or entecavir: harder administration (injection vs pill), higher cost, and more side effects. These side effects are so inconvenient for the patient that IFN treatment usually stops after one year.

Mathematical models have proven useful for the understanding of virus and drug dynamics under drug therapy in infections such as human immunodeficiency virus (HIV), hepatitis C (HCV), and HBV [16, 32, 14, 39, 35, 9, 21]. To get a better understanding of the virus-host dynamics, studies have combined clinical data with mathematical models. For example, Guidotti *et al.* [7] showed that a strong immune response is the key to overcome the disease. Similar studies have been made to understand the efficacy of drugs in curing hepatitis B. For instance, Lewin *et al.* [44] have estimated 95% lamivudine efficacy in blocking new virus production which can be increased to 99% when combined with famciclovir.

Clinical data has shown that, in the case of HBV patients undergoing therapy, most of the virus decay profiles are biphasic [35, 9, 21]. Mathematical models applied to such data have shown that for some patients drug therapy yields fast clearance of the virus whereas for other

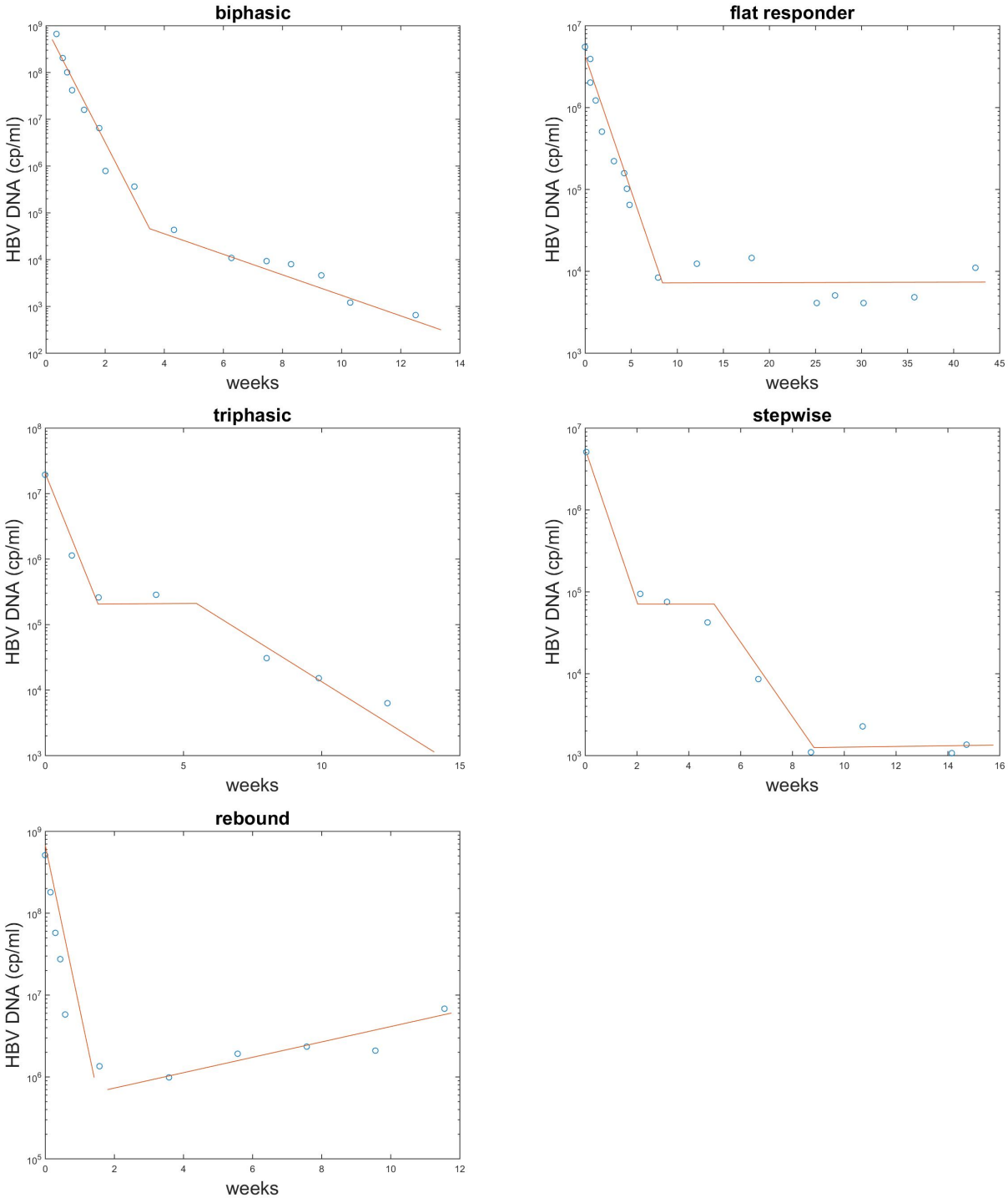

Figure 2.1: Different virus decay profiles observed in patients. [41]

patients the clearance is much slower [44]. Moreover, for some patients, the decay pattern

of HBV DNA is more complex than the usual biphasic pattern [44]. As mentioned above, in some cases treatment needs to be stopped. Then viral relapse is observed in most patients. In figure 2.1, the circles represent the data from different patients and the lines suggest the kind of virus behavior we observe. The kind of therapy and the studies they were taken from in patients A-E are sumarize in table 2.1

Figure	Therapy	Reference
A	lamivudine, famciclovir	[44]
B	pegylated interferon-α2a	[15]
C	adefovir dipivoxil	[21]
D	lamivudine, famciclovir	[44]
E	lamivudine	[44]

Table 2.1: Therapy in patients from figure 3.3

In this thesis, we want to get a better understanding of the mechanisms behind the complex virus dynamics seen during drug therapy in HBV infections. Such knowledge may help improve treatment, by informing what drugs to use, when to start and when to stop.

Chapter 3

Mathematical background

3.1 Introduction

Mathematical models have been used in life sciences to interpret experimental data, to understand the processes that produced that data, and even to test hypotheses and make predictions [40]. In 1760 Daniel Bernoulli introduced the first mathematical method into the field of epidemiology which showed that vaccination against smallpox was advantageous for protection [4, 2]. Bernoulli's results motivated the incorporation of mathematical models into biological studies. In the field of epidemiology, mathematical modeling gave valuable insight into the spread of a disease among humans and provided hypotheses for developing strategies to control it. Nowadays mathematical models can describe the details of the chemistry in a living being: interactions between pathogens, host cells, and immune system [28, 27]. Great progress has been made towards understanding biological processes at the cellular level but there are still complex mechanisms that need of more sophisticated models in order to be completely understood [38].

3.2 Models of HBV infection

Mathematical modeling is a useful tool in the study of virus dynamics because it helps to interpret the experimental results and to understand the underlying biological mechanisms involved. The field of hepatitis B infection, in particular, has adopted it as an alternative way of extracting information regarding virus characteristics, drug efficacy and immune responses [38, 35, 21, 44, 41, 42]. Below, we summarize some of the models relevant for this thesis.

The simplest version of an in-host model for the interaction between liver cells (uninfected and infected) and the virus is the one derived from diagram 3.1. Here T represents the target uninfected cells (uninfected hepatocytes), I represents the infected cells (infected

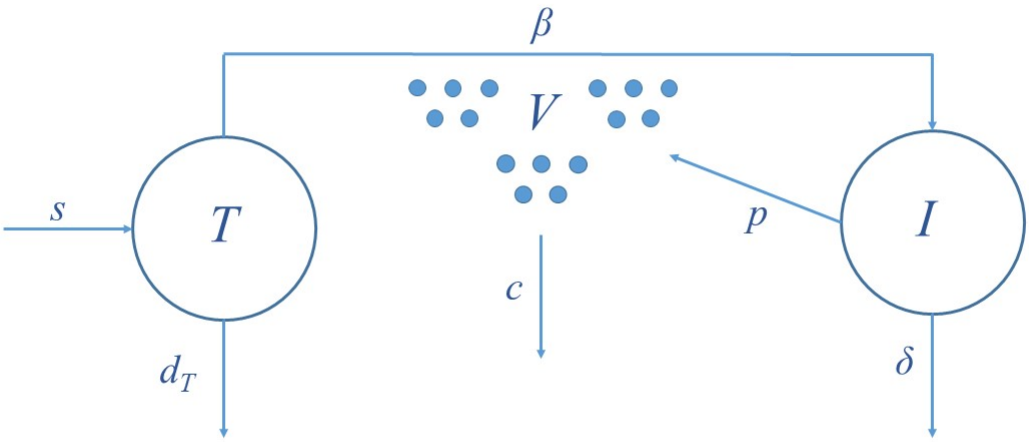

Figure 3.1: Diagram for the basic virus dynamics model

hepatocytes), and V represents the hepatitis B virus. This model was introduced by Perelson [38] for the study of HIV infection and first used in HBV by Nowak *et al.* [35]. It considers that target cells are infected at rate β and infection occurs by contact between target cells and virus. It also assumes that infected cells die at a rate δ and produce virus at a rate p. The virus dies at rate c. The liver produces new target cells and these may die before being infected. We use s and d_T to denote the constant production rate and the natural death rate, respectively. Under this assumptions the model becomes

$$\begin{aligned} \frac{dT}{dt} &= s - \beta VT - d_T T, \\ \frac{dI}{dt} &= \beta VT - \delta I, \\ \frac{dV}{dt} &= pI - cV. \end{aligned}$$

In any mathematical model, stability analysis gives a general idea on how the model will behave at equilibrium. This model has two equilibrium points, one in which the virus goes extinct and one in which the virus persists. The measure that determines whether the virus will disappear or not is called the basic reproductive number R_0, and it represents the number of new viruses arising from one virion in a naive target population. If $R_0 < 1$ we have stability of the disease free steady state, meaning virus and infected cell populations will die out; if $R_0 \geq 1$ the infection persists. The analysis in [35] shows that the basic reproductive ratio R_0 is given by

$$R_0 = \frac{s\beta p}{\delta d_T c}.$$

This model predicts clearance of the virus for patients with strong antibody mediated immune responses against free virus (high c) or strong cellular immune responses against infected cells (high δ).

Nowak *et al.* [35] fitted this model to HBV patients under lamivudine treatment under the assumption that the therapy inhibits virus production completely. In terms of the model, this implies that

$$\frac{dV}{dt} = -cV,$$

and the virus decays exponentially, $V(t) = V_0 e^{-ct}$. This assumption was good for modeling short term therapy but would not fit the virus data after a certain period of time. So an improvement to their model was introduced by Tsiang *et al.* [21]. The new model does not assume complete efficacy of the drug. Instead it introduces a new parameter ϵ to represent the efficacy of the treatment on blocking virion production. The parameter range is $0 \leq \epsilon \leq 1$, where $\epsilon = 0$ means therapy has no effect on blocking virus production, and $\epsilon = 1$ means therapy completely blocks virus production. The model becomes

$$\begin{aligned} \frac{dT}{dt} &= s - \beta VT - d_T T, \\ \frac{dI}{dt} &= \beta VT - \delta I, \\ \frac{dV}{dt} &= (1-\epsilon) pI - cV, \end{aligned}$$

with new basic reproductive number

$$R_0 = (1-\epsilon)\frac{s\beta p}{\delta d_T c}.$$

As before, when $R_0 < 1$ the virus is cleaned. Therefore a big ϵ will account for viral clearance. This model was applied to data from a large number of drug trials. HBV infected patients, after the start of therapy, showed biphasic decay of the virus, most common behavior seen in drug trials and treatments [35, 44, 21]. Some patients, however, show a more complex viral decay with one or several shoulder phases before clearance. Lewin *et al.* [44] introduce some changes in the model that predicted these special decays. Unlike HIV infected cells, infected hepatocytes have the ability to recover due to the fact that the virus does not integrate, and therefore can be eliminated. They denote this recovery rate by ρ. This was included in [44] together with another parameter η which represents the efficacy of the drug in blocking infection. Analogously to ϵ, the range for η is $[0, 1]$. The model becomes

$$\begin{aligned} \frac{dT}{dt} &= s - (1-\eta)\beta VT - d_T T + \rho I, \\ \frac{dI}{dt} &= (1-\eta)\beta VT - \delta I - \rho I, \\ \frac{dV}{dt} &= (1-\epsilon) pI - cV, \end{aligned}$$

and the new basic reproductive number becomes

$$R_0 = (1-\epsilon)(1-\eta)\frac{s\beta p}{d_T c(\rho+\delta)}.$$

When $R_0 < 1$ the virus will go extinct. Otherwise it persists.

As mentioned before, these HBV models evolved from models meant for HIV. But there are important biological differences between HBV and HIV infections. For instance, most HBV patients clear the virus under a strong immune response against the virus. A model that does not account for drug therapy but that includes some of the important biological features characteristic of HBV was introduced by Ciupe *et al.* [43]. A summary of the relations and parameters included in this model is shown on diagram 3.2. Ciupe *et al.* [43] consider target cells T, productively infected cells I, free virus V, immune effector cells E, and refractory cells R. The effector cells represent immune cells capable of both killing and curing infected cells. The population of refractory cells consists of recovered infected cells that can no longer be infected or infected cells which do not produce a measurable amount of virus. Hepatocytes proliferation is described by a logistic term with maximum proliferation rate r and carrying capacity K. When target cells T are infected, they move into the infected cells population I. Infected cells produce new virus at rate p and can either recover at rate ρ or die due to killing by the effector cells E at rate μ. The effector cells are at steady state s/d_E before infection. Effector cells expand at rate α. The expansion is delayed. We model this, which is modeled by a delay differential equation with interaction between I and E leading to E expansion τ days later. The equations corresponding to this model are:

$$\begin{aligned}
\frac{dT}{dt} &= rT\left(1-\frac{T+I+R}{K}\right) - \beta VT + \rho_R R,\\
\frac{dI}{dt} &= rI\left(1-\frac{T+I+R}{K}\right) + \beta VT - \rho IE - \mu IE,\\
\frac{dV}{dt} &= pI - cV,\\
\frac{dE}{dt} &= s + \alpha I(t-\tau)E(t-\tau) - d_E E.\\
\frac{dR}{dt} &= \rho IE + rR\left(1-\frac{T+I+R}{K}\right) - \rho_R R - \mu_1 RE
\end{aligned}$$

This model is used to show the transition between acute and chronic hepatitis B disease. It shows that the virus is cleared for strong immune response that cures cells and makes them refractory to reinfection.

Dahari *et al.* [41] considers a simplified version of the model from Ciupe *et al.* [43] by assuming interactions between target cells, one population of infected cells and the virus population. To account for liver regeneration through rapid cell division, Dahari *et al.* [41]

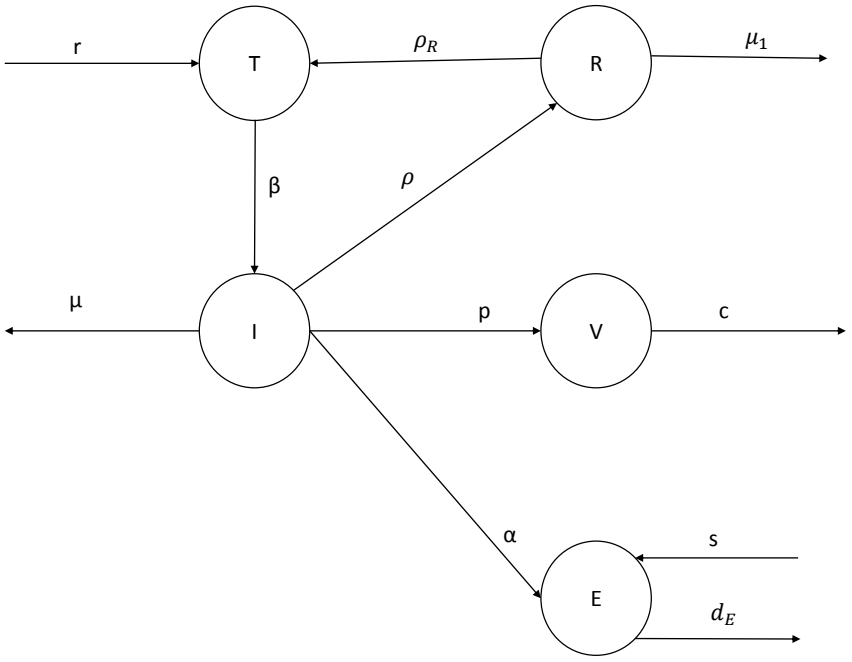

Figure 3.2: Diagram of the virus dynamics for the model accounting for two infected cell populations and immune system effector cells.

included the proliferation of both target cells and infected cells, r_T and r_I respectively. This proliferation was modeled by a logistic term, with per capita division at rates r_T and r_I, and carrying capacity K. Lastly, Dahari *et al.* [41] applied this model for the investigation of drug treatment with η drug efficacy in blocking infection and ϵ grud efficacy in bloking virion production. The model is:

$$\frac{dT}{dt} = s + r_T T\left(1 - \frac{T+I}{K}\right) - \beta(1-\eta)VT - d_T T + \rho I, \tag{3.1}$$

$$\frac{dI}{dt} = r_I I\left(1 - \frac{T+I}{K}\right) + \beta(1-\eta)VT - (\delta+\rho)I, \tag{3.2}$$

$$\frac{dV}{dt} = (1-\epsilon)pI - cV, \tag{3.3}$$

and forms the basis of this thesis.

The addition of proliferative term in equations (3.1)-(3.2) is needed to account for rich behavior observed among patients undergoing drug therapy. Among the observed virus behavior are biphasic decays, triphasic decays, flat second phase, and rebound. Dahari *et al.* [41] has considered several drug trials that show rich dynamics of viral decay. Results from fitting the model to data in each pattern are shown on figure 3.3. In figure 3.3, the experimental data is from figure 2.1 and the corresponding parameter values are in table 3.1.

The data points in the figures are from Dahari *et al.* [41]. In the paper they also provide the parameter values that fit such data. We use those parameter values to generate the corresponding model's solution and observe that indeed the model can predict the different decay profiles.

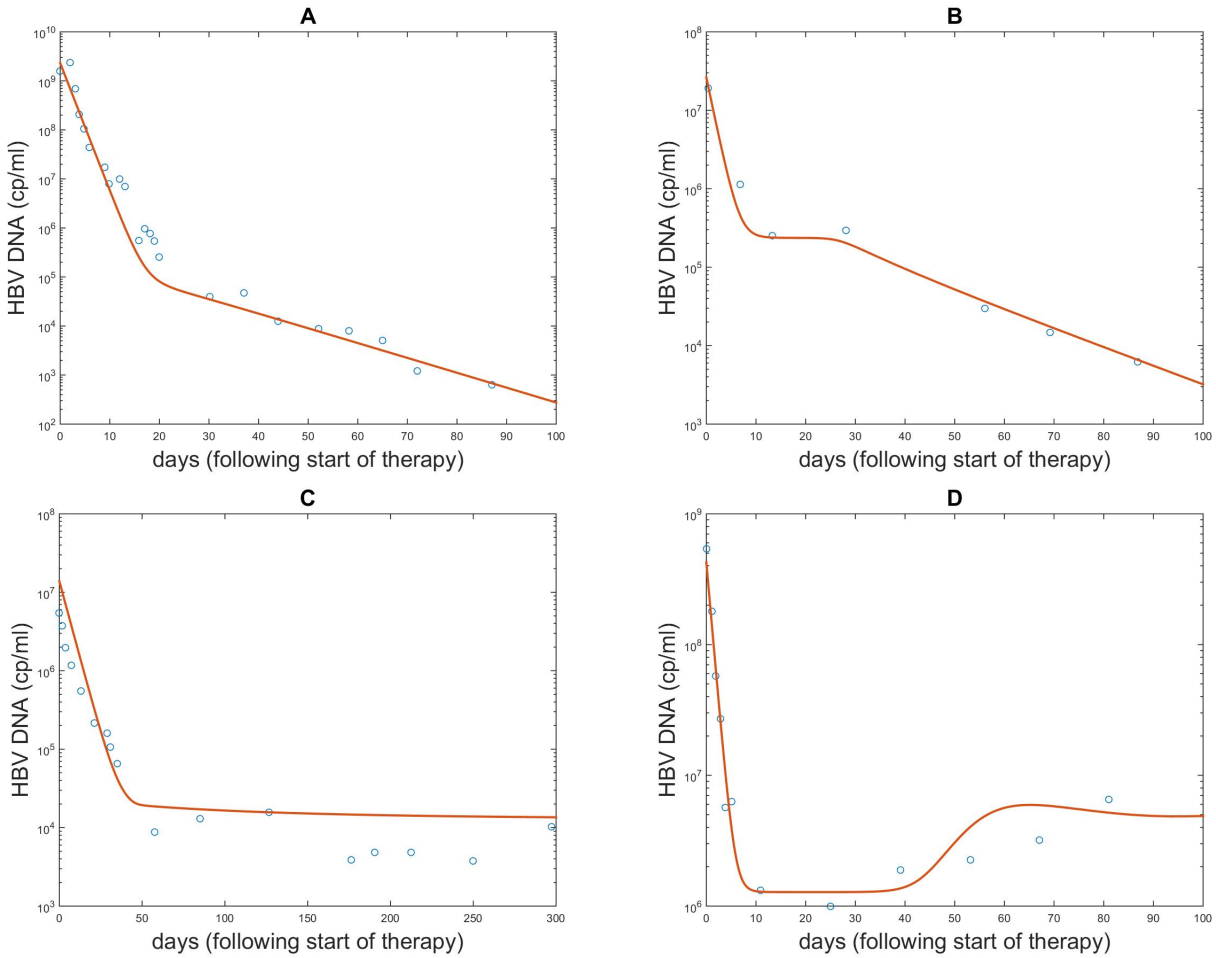

Figure 3.3: Model (3.1)-(3.3) rise to different profiles.

Figure	s	d_T	β	r_T	r_I	K	δ	ρ	p	c	η	ϵ
A	1	0.01	1×10^{-10}	3	0.6	1.9×10^7	0.07	0	100	0.67	0.5	0.99934
B	1	2.7×10^{-3}	2.5×10^{-7}	0.9	0.2727	1.9×10^7	0.22	0	5	0.7	0.5	0.991
C	1	5.3×10^{-3}	1.9×10^{-6}	0.8	0.2759	1.9×10^7	0.25	0	1.4	0.18	0.2	0.9988
D	1	9×10^{-4}	6.6×10^{-8}	0.5	0.0694	1.9×10^7	0.06	0	164	1	0.5	0.997

Table 3.1: Parameter values in figure 3.3

Chapter 4

Numerical background

It is well known that observation and theory are the two classical pillars of science. Over the years, a new field of study has been developed and is considered now as the third pillar of science. Such field is the computational science. The contribution of this new discipline is its ability to use algorithms to simulate mathematical models. These algorithms can reconstruct past events using inverse analysis or they can predict future outcomes given certain incomes. Computational science can also illustrate complicated mechanisms, giving the researchers a better opportunity to make and test hypotheses. For example, in the field we are focusing here, viral dynamics, Institute for Computational Engineering and Sciences in University of Texas has simulated the behavior of the HIV RT protein and this has helped researchers to design therapeutic drugs [12].

In this thesis, we study a mathematical model for hepatitis B virus dynamics. This model depends on 12 parameters, and the behavior of the model depends on the values of these parameters. Our goal is to find the relationship between the parameter values and the outcome of the system. In chapter 6, we will use numerical methods to try to attain this goal. These numerical methods are based on forward modeling, which is widely use in geophysics [52]. While an inverse problem obtains the values of the parameters that would explain the data collected, forward modeling consists on using known values of parameters to predict the outcome of the corresponding system. In addition to predicting the data, a forward model should also explain how that data is generated. A more rigorous definition of these concepts follows.

Consider a system

$$\frac{d\vec{x}}{dt} = f(\vec{x}, \theta, t)$$

where $\vec{x}$ is the time dependent state variable, θ are the parameters of the system and f is the function that describes the change in the state variable.

Definition. Given a data set $\vec{x}_d$, finding a value θ^* of the parameter domain such that the

solution of

$$\frac{d\vec{x}}{dt} = f(\vec{x}, \theta^*, t)$$

fits $\vec{x}_d$ represents an inverse problem.

Definition. Given the value of the parameters θ_d of the model, a *forward problem* predicts certain properties of the solution $\vec{x}$ of

$$\frac{d\vec{x}}{dt} = f(\vec{x}, \theta_d, t). \tag{4.1}$$

When using numerical methods, we always need to know how accurate our results are. Verification and Validation studies (V& V) [46] help to establish how good a numerical simulation is. Part of the validation process consists on comparing the numerical predictions with actual data by taking in account experimental uncertainties and errors. Uncertainty quantification (UQ) gives error bars to the predictions made by numerical simulations. Another goal of UQ is to know what are the chances that a certain outcome actually happens. Such knowledge gives a better understanding of risks taken when making a decision based UQ analysis. For example, uncertainty analysis was used in 1994 by Blower and Dowlatabadi to study the behavior of a deterministic model of HIV transmission [11]. They determined the imprecision of the solution $\vec{x}$ of (4.1) due to uncertainty on the parameters θ_d estimation.

When investigating a model's predictions numerically, it is important to note the difference between errors and uncertainties. The American Institute of Aeronautics and Astronautics (AIAA) [37] defines "error" as known deficiencies of the models or algorithms used and "uncertainties" as a potential deficiency due to lack of knowledge. UQ focuses on characterizing and reducing the uncertainties in applications, i.e., tries to determine how likely an outcome is if some aspects of the system are not exactly known.

Uncertainties can be classified in two types: aleatory and epistemic [24]. The first is the physical variability of the system under analysis. Epistemic uncertainty is potential deficiency due to lack of knowledge. Epistemic uncertainty can arise from assumptions leading to simplifications of the model of physical process under investigation.

When developing a mathematical model there are several simplifications or assumptions that need to be made. When using numerical methods to analyze the model, a discretization is introduced. Finally, when including uncertainty in a study, the analysis of such models becomes more difficult. There are three main steps on this process: data assimilation, uncertainty propagation and certification. Data assimilation focuses on characterizing specific inputs, such as parameters, needed to simulate the model. There are several approaches on how to find these values [10, 51, 25]. With probabilistic approaches, the goal is to determine a probability distribution function (PDF) [47] for each input quantity. Once this is accomplished, uncertainty propagation study will determine the PDF of the output quantities. Once the statistics are determined for each quantity of interest, validation is performed [3].

In this thesis, UQ would be used to study forward uncertainty propagation. This is the quantification of uncertainties in system output due to parametric variability. The goals are to evaluate the reliability of the outputs and asses their probability distribution, and the methods used to attain this goals are simulation-based methods such as Monte Carlo simulations [1].

A type of Monte Carlo simulation is rejection sampling, also known as acceptance-rejection method. It is a simple technique used to generate observations from a distribution. The idea is running simulations a lot of times to get the distribution of the variable under study. It works for any distribution in $\mathbb{R}^m$ and it relies on the fact that when sampling a random variable, we only need to uniformly sample from the region of values it takes.

In these thesis, we are looking at qualitative outcomes such as virus decay profiles, and quantitative outcome such as time until virus clearance. In chapter 6, we define our parameters PDFs by bounding their values between a maximum and a minimum and assuming they are all equally probable. Then we choose the number N of simulations, generate N random samples of parameter values, and classify them in terms of the output observed. We will separate: stable from unstable behavior; biphasic viral decay from triphasic viral decay; and fast from slow clearance.

Chapter 5

Analytical results

In this chapter, we describe the Dahari *et al.* model [41] on several levels. We start by explaining the derivation. Then we perform stability analysis and give numerical results. Lastly, we derive ways to characterize the parameter regions for the four different patterns observed in the data.

The model is defined by equations (3.1)-(3.3) [41]. They consider three populations: uninfected hepatocytes or target cells T, infected cells I, and free virus V. The target cells are produced at a constant rate s, die at a constant rate d_T, and are infected by the virus at rate β. Infected cells recover at rate ρ due to non-cytopathic immune responses [50], die at rate δ due to cytopathic killing [7] and produce new virus at rate p. Both target and infected cells proliferation is modeled by a logistic term with per capita maximal growth rates r_T and r_I and carrying capacity K. The virus clearance is denoted by c. Dahari *et al.* [41] assume that therapy with IFN and nucleot(s)ide analogs suppress virus replication by a factor $(1-\epsilon)$ where ϵ is the efficacy of drug in blocking virus production. Lewin *et al.* [44] consider that lamivudine blocks target cell infection by a factor of $(1-\eta)$. The following equations and table 5.1 summarize the assumptions:

$$\frac{dT}{dt} = s + r_T T\left(1 - \frac{T+I}{K}\right) - \beta(1-\eta)VT - d_T T + \rho I, \tag{5.1}$$

$$\frac{dI}{dt} = r_I I\left(1 - \frac{T+I}{K}\right) + \beta(1-\eta)VT - (\delta+\rho)I, \tag{5.2}$$

$$\frac{dV}{dt} = (1-\epsilon)pI - cV. \tag{5.3}$$

Note that the range of values for both ϵ and η is $[0,1]$.

Our goal now is to find the relationship between the parameters in the model and the patterns observed in the patient data: biphasic decay, triphasic decay, and rebound.

Parameter	Description	Units
s	constant hepatocyte production	cell day^{-1} mL^{-1}
d_T	hepatocyte death rate	day^{-1}
β	infectivity rate	mL virions^{-1} day^{-1}
r_T	growth rate of hepatocytes	day^{-1}
r_I	growth rate of infected hepatocytes	day^{-1}
K	liver size	cells mL^{-1}
δ	killing rate of infected hepatocytes	day^{-1}
ρ	recovery rate	day^{-1}
p	virus production	virions cell^{-1} day^{-1}
c	virus clearance	day^{-1}
η	effectiveness of therapy in blocking infection	
ϵ	effectiveness of drug in blocking virion production	

Table 5.1: Parameters of the model.

5.1 Initial condition

We will consider the infected steady state of the model without treatment as our initial condition [26]. The equations defining such model are similar to (5.1)-(5.3); the only difference is that the parameters due to drug therapy are zero, i.e., $\eta = 0$ and $\epsilon = 0$ simplifying the system to

$$\frac{dT}{dt} = s + r_T T\left(1 - \frac{T+I}{K}\right) - \beta V T - d_T T + \rho I, \tag{5.4}$$

$$\frac{dI}{dt} = r_I I\left(1 - \frac{T+I}{K}\right) + \beta V T - (\delta + \rho) I, \tag{5.5}$$

$$\frac{dV}{dt} = pI - cV. \tag{5.6}$$

Observe that the disease-free steady state is the same as for the model with therapy $E_1 = (T_1, 0, 0)$ where

$$T_1 = \frac{K}{2r_T}\left(r_T - d_T + \sqrt{(r_T - d_T)^2 + 4\frac{sr_T}{K}}\right).$$

The infected steady state $E_0 = (T_0, I_0, V_0)$ is given by

$$\frac{\beta p}{c}\left(1 - \left(\frac{r_T}{r_I} + \frac{\beta p K}{c r_I}\right)\right) T_0^2 + \left(\delta\left(\frac{r_T}{r_I} + \frac{\beta p K}{c r_I}\right) - d_T - \frac{\beta p K}{c}\right) T_0 + s = 0,$$

$$I_0 = \left(\frac{\beta p K}{c r_I} - 1\right) T_0 + K\left(1 - \frac{\delta}{r_I}\right),$$
$$V_0 = \frac{p}{c} I_0.$$

which exists for $c(r_I - r_T) - \beta p K < 0$. In general, $r_I < r_T$ so this condition is easily satisfied. We use this as initial condition for the model (5.1)-(5.3).

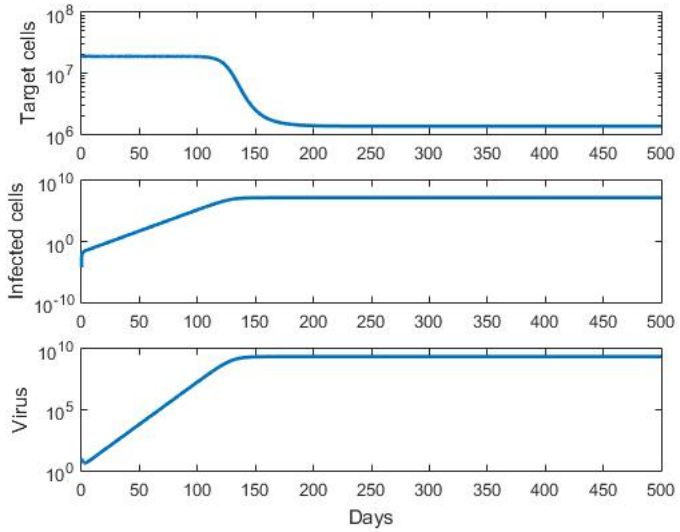

Figure 5.1: Behavior of the model without therapy for $s = 1, \rho = 0, K = 1.9 \times 10^7, d_T = 0.01, p = 100, c = 0.67, \beta = 10^{-10}, r_T = 3, r_I = r_T/5, \delta = 0.07$.

In figure 5.1 we show a case in which, without therapy, the virus does not clear. So predictions about the result of therapy would be made simulating model (5.1)-(5.3) with initial condition being the final state observed.

5.2 Properties of the solution

In this section we will consider the system (5.1)-(5.3) subject to initial conditions

$$T(0) = T_0 > 0, \qquad I(0) = I_0 > 0, \qquad V(0) = V_0 > 0, \qquad T(0) + I(0) \leq K. \tag{5.7}$$

Proposition 1. *The solution $V(t)$ of (5.1)-(5.3) subject to (5.7) is positive on $[0, b)$ for some $b > 0$.*

Proof. The partial derivatives of the right hand side of our system are bounded around $t = 0$. Therefore the system is locally Lipschitz at $t = 0$ and solution exists and is unique on $[0, b)$ for some $b > 0$. Assume that there exists $t_1 \in (0, b)$ such that $V(t_1) = 0$ and all variables are positive on $[0, t_1)$. Then for all $t \in [0, t_1]$

$$\frac{dV}{dt} = (1 - \epsilon)pI - cV \geq -cV,$$

and so

$$V(t_1) \geq V_0 e^{-ct_1} > 0,$$

a contradiction. Then $V(t) > 0$ for all $t \in [0, t_1]$.

□

Proposition 2. *If* $\max\{r_T, r_I\} > \min\{d_T, \delta\}$*, then the solution* $(T(t), I(t))$ *of* (5.1)-(5.3) *subject to* (5.7) *remains bounded on* $[0, b)$ *for some* $b > 0$*.*

Proof. Let $F(t) = T(t) + I(t)$. Then

$$\frac{dF}{dt} = s + (r_T T + r_I I)\left(1 - \frac{F}{K}\right) - d_T T - \delta I. \tag{5.8}$$

Consider (5.8), let $r_{max} = \max\{r_T, r_I\}$ and let $d_{min} = \min\{d_T, \delta\}$. Then

$$\begin{aligned}
\frac{dF}{dt} &\leq s + r_{max} F\left(1 - \frac{F}{K}\right) - d_{min} F \\
&= s + (r_{max} - d_{min})F - \frac{r_{max}}{K} F^2 \\
&= -\frac{r_{max}}{K}(F - X)(F - Y),
\end{aligned}$$

where

$$X = \frac{r_{max} - d_{min} + \sqrt{(r_{max} - d_{min})^2 + \frac{4sr_{max}}{K}}}{-2s},$$

$$Y = \frac{r_{max} - d_{min} - \sqrt{(r_{max} - d_{min})^2 + \frac{4sr_{max}}{K}}}{-2s}.$$

Then

$$\int \frac{dF}{(F-X)(F-Y)} \leq \int -\frac{r_{max}}{K} dt$$

$$\frac{1}{X-Y} \ln|F-X| + \frac{1}{Y-X} \ln|F-Y| \leq -\frac{r_{max}}{K} t$$

$$\left|\frac{F-X}{F-Y}\right| \leq \exp\left(-\frac{(X-Y)r_{max}}{K} t\right).$$

and, since $r_{max} > d_{min}$,

$$F(t) \leq \frac{X - Y\exp\left(-\frac{(X-Y)r_{max}}{K}t\right)}{1 - \exp\left(-\frac{(X-Y)r_{max}}{K}t\right)}.$$

Note that $X - Y > 0$, and so $F(t)$ is bounded. Since $T(t)$ and $I(t)$ are positive on $(0, b)$ we obtain that $T(t)$ and $I(t)$ are bounded.

□

Proposition 3. *The solution* $(T(t), I(t))$ *of* (5.1)-(5.3) *subject to* (5.7) *is positive on* $[0, b)$ *for some* $b > 0$.

Proof. We use F to show that T and I are positive.

Consider (5.8), let $r_{min} = \min\{r_T, r_I\}$ and let $d_{max} = \max\{d_T, \delta\}$. Assume that there exists $t_1 \in (0, b)$ such that $F(t_1) = 0$ and all variables are positive on $[0, t_1)$. Assume also that T and I are bounded on $[0, t_1)$, i.e., there exist M_1 and M_2 such that $T(t) \leq M_1$ and $I(t) \leq M_2$ for all $t \in [0, t_1)$. Then for all $t \in [0, t_1]$

$$\begin{aligned}\frac{dF}{dt} &\geq r_{min}F\left(1-\frac{F}{K}\right)-d_{max}F \\ &\geq r_{min}F\left(-\frac{M_1+M_2}{K}\right)-d_{max}F \\ &= -\tilde{c}F, \qquad\qquad \tilde{c}>0\end{aligned}$$

and so

$$F(t_1) \geq F_0 e^{-\tilde{c}t_1} > 0$$

a contradiction. Then $F(t) > 0$ for all $t \in [0, t_1]$. Since we assume all the variables positive on $[0, t_1)$, this implies that both $T(t)$ and $I(t)$ are positive for all $t \in [0, t_1]$.

□

Proposition 4. *If* $\max\{r_T, r_I\} > \min\{d_T, \delta\}$*, then the solution* $V(t)$ *of* (5.1)-(5.3) *subject to* (5.7) *remains bounded on* $[0, b)$ *for some* $b > 0$*.*

Proof. If $I(t)$ is bounded on $[0, b)$, then there exists a number $M > 0$ such that

$$M \geq (1-\epsilon)p \sup_{t\in[0,b)} I(t).$$

Then for any $t \in [0, b)$ we have

$$\frac{dV}{dt} = (1-\epsilon)p - cV \leq M - cV,$$

and so

$$V(t) \leq \max\left\{V_0, \frac{M}{c}\right\}.$$

□

5.3 Stability analysis

System (5.1)-(5.3) has two steady states: the disease-free steady state $E_1 = (T_1, 0, 0)$ with

$$T_1 = \frac{K}{2r_T}\left(r_T - d_T + \sqrt{(r_T - d_T)^2 + 4\frac{sr_T}{K}}\right);$$

and the infected steady state $E_2 = (T_2, I_2, V_2)$ with

$$T_2^2\frac{AD}{Kr_I} - T_2\left(r_T B - d_T - A(1-B) + \rho\left(\frac{A}{r_I} - 1\right)\right) - \rho K(1-B) - s = 0$$

$$I_2 = \left(\frac{A}{r_I} - 1\right)T_2 + (1-B)K, \text{and}$$

$$V_2 = (1-\epsilon)\frac{p}{c}I_2,$$

where $A = (1-\eta)(1-\epsilon)\beta\frac{p}{c}K$, $B = \frac{\delta+\rho}{r_I}$, and $D = A + r_T - r_I$.

In order for the disease to disapear, we need the first steady state E_1 to be stable. To find the conditions that guarantee the stability of E_1, we impose that the eigenvalues of the corresponding Jacobian matrix have negative real parts.

Proposition 5. *The free disease steady state is locally asymptotically stable if $R_0 < 1$, where*

$$R_0 = \frac{(1-\epsilon)(1-\eta)p\beta T_1}{c(\rho+\delta)} + \frac{r_I\left(1 - \frac{T_1}{K}\right)}{\rho+\delta} \tag{5.9}$$

Proof. The Jacobian matrix for the system is

$$J = \begin{pmatrix} r_T\left(1 - \frac{2T+I}{K}\right) - \beta(1-\eta)V - d_T & -r_T\frac{T}{K} + \rho & -\beta(1-\eta)T \\ -r_I\frac{I}{K} + \beta(1-\eta)V & r_I\left(1 - \frac{T+2I}{K}\right) - \rho - \delta & \beta(1-\eta)T \\ 0 & (1-\epsilon)p & -c \end{pmatrix},$$

which evaluated at E_1 becomes:

$$J = \begin{pmatrix} r_T - d_T - 2r_T\frac{T_1}{K} & -r_T\frac{T_1}{K} + \rho & -\beta(1-\eta)T_1 \\ 0 & r_I - r_I\frac{T_1}{K} - \rho - \delta & \beta(1-\eta)T_1 \\ 0 & (1-\epsilon)p & -c \end{pmatrix},$$

has eigenvalues

$$\lambda_1 = -\sqrt{(r_T - d_T)^2 + 4\frac{sr_T}{K}}$$

$$\lambda_{2,3} = \frac{r_I - c - \delta - \rho}{2} - \frac{r_I}{2}\frac{T_1}{K} \pm \sqrt{\frac{(c+\delta+\rho-r_I)^2}{4} + (1-\eta)(1-\epsilon)\beta p T_1 + c\left(r_I - \delta - \rho - r_I\frac{T_1}{K}\right)}$$

Note that λ_1 is always negative and, if $R_0 < 1$, then $\lambda_{2,3}$ are also negative.

□

Proposition 6. *E_2 is locally asymptotically stable when $R_0 > 1$.*

Proof. The proof is messy. We present numerical examples in Figure 5.2.

□

As sown in 5.2, when $R_0 > 1$ virus persists whereas if $R_0 < 1$ virus goes extinct.

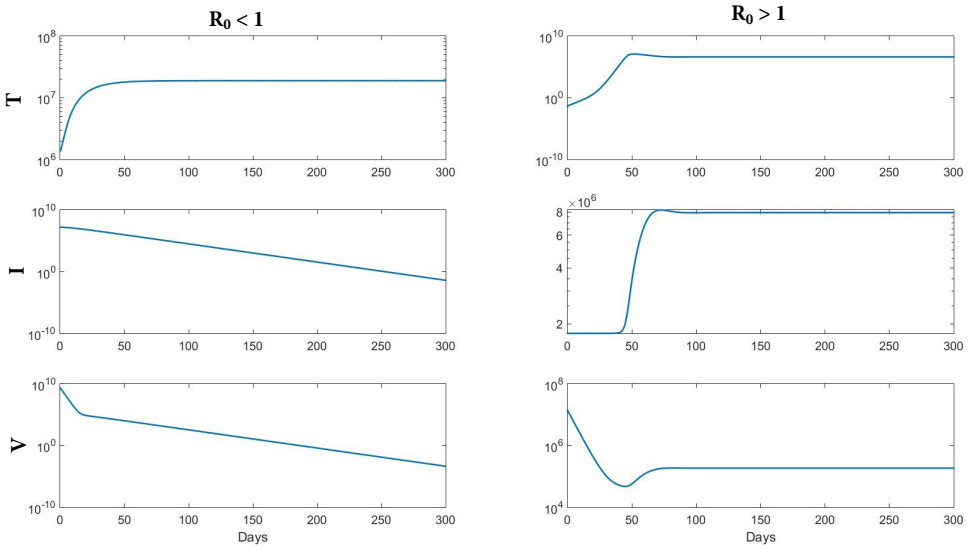

Figure 5.2: We observe extinction of the virus when $R_0 < 1$ and persistance of the virus when $R_0 \geq 1$. Left: $R_0 = 1.3716 \times 10^{-4}$. Right: $R_0 = 2.6973$.

5.4 Drug efficacy

Our stability results obtained in the previous section stated in terms of a *critical drug efficacy* [41]. The overall drug efficacy ϵ_{tot}, that combines the effectiveness of therapy in blocking infection and virion production, is

$$1 - \epsilon_{tot} = (1 - \eta)(1 - \epsilon).$$

The critical drug efficacy is

$$\epsilon_c = 1 - \frac{c((\delta + \rho)K + r_I(T_1 - K))}{p\beta K T_1}.$$

If $\epsilon_{tot} > \epsilon_c$, then the model predicts clearance of the virus. This condition is equivalent to our $R_0 < 1$ condition. Dahari *et al.* argue that the model not only predict clearance of the virus for $\epsilon_{tot} > \epsilon_c$ but the decay is continuous, meaning it will be a biphasic or triphasic decay. If $\epsilon_{tot} < \epsilon_c$ then therapy is not efficient enough and so flat phases and rebounds may occur.

5.5 Analytical approximation of the solution

The goal of this research is to find parameter regions that explain the differences seen in the data from patients undergoing combination therapy, in particular the biphasic and triphasic patterns. Since we have a good analytical understanding of what parameters allow for V to go extinct, i.e. $R_0 < 1$, we first investigated if the local linear approximation of the solution at $V = 0$, $I = 0$, $T = T_1$ can match the non-linear solution. Briefly, the linear approximation around $(T_1, 0, 0)$ has the form:

$$V(t) = c_1 e^{\lambda_1 t} + c_2 e^{\lambda_2 t} + c_2 e^{\lambda_2 t}$$

where

$$\lambda_1 = -r_T - d_T$$

$$\lambda_2 = \frac{-(\rho + c + \delta) + \sqrt{(\rho + c + \delta)^2 - 4(\rho + \delta)c + 4\beta pK(1 - \epsilon)(1 - \eta)}}{2}$$

$$\lambda_3 = \frac{-(\rho + c + \delta) - \sqrt{(\rho + c + \delta)^2 - 4(\rho + \delta)c + 4\beta pK(1 - \epsilon)(1 - \eta)}}{2}$$

If $|\lambda_1| \neq |\lambda_2| \approx |\lambda_3|$, then we would expect to observe a biphasic decay. If $|\lambda_2| = 0$ and $|\lambda_3| < |\lambda_1|$ then we expect to see a triphasic decay with a flat region.

The length D_1 of the first phase decay is given by the time at which the curves $c_1 e^{\lambda_1 t}$ and $c_2 e^{\lambda_2 t}$ intersect

$$D_1 = \frac{\ln c_2 - \ln c_1}{\lambda_1 - \lambda_2}.$$

Similarly, the duration D_2 of the second phase is

$$D_2 = \frac{\ln c_3 - \ln c_2}{\lambda_2 - \lambda_3}.$$

To calculate the length D_3 of the third phase, consider certain tolerance τ under which the virus is assumed to be extinct. Then

$$D_3 = \frac{\ln \tau - \ln c_3}{\lambda_3}.$$

Here $\tau = 3 \times 10^{-4}$ per mL. Briefly, a 70kg person has on average 3L of blood. We normalize 1 virion in that concentration to get the limit of extinction of V to be 1/3L$= 3 \times 10^{-4}$ virion per mL.

The linear approximation approach was used by Lewin *et al.* [44]. This method is sometimes useful for determining the slopes of the two or three phase decay. Indeed, in figure 5.3 the slope of the first decay is -0.7 and λ_3 is -0.6703. For most cases, however, the linear approximation is not a good proxy for the length of the decay. Indeed, in figure 5.3 $D_3 = 43.8$ Since we want to determine general conditions for biphasic vs. triphasic patterns, we will approach this using numerical methods.

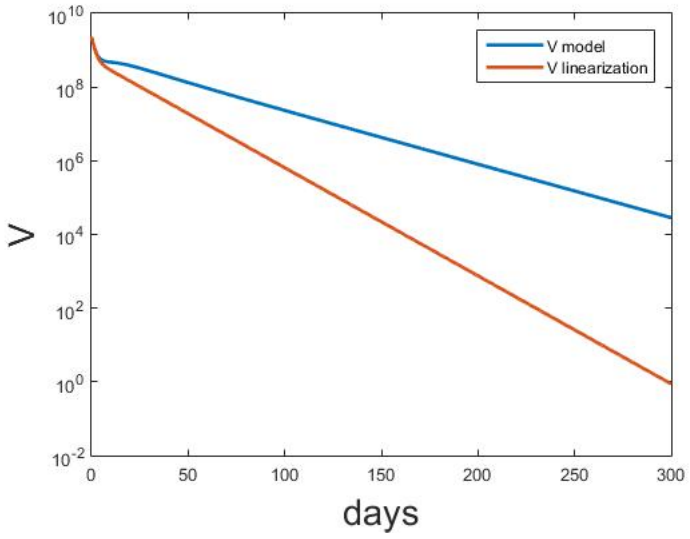

Figure 5.3: Parameter values as in table 6.1 with $r_T = 1.49, r_I = 0.386, \delta = 0.0679, \epsilon = 0.785$.

Chapter 6

Numerical results

The analytical results are sufficient for separating the virus decay from virus rebound. Indeed, as seen in section 5.1, for $R_0 > 1$ the virus rebounds, while for $R_0 < 1$, virus goes extinct (see figure 5.2). The analytical results cannot, however, tell us what kind of extinction or persistent patterns are obtained. In this chapter, we derive a numerical method for investigating this using the techniques described in chapter 4. We will start by determining the parameters that give viral extinction.

Since we know that the virus will go extinct when $R_0 < 1$, we looked for the behavior of the model when varying all the parameters satisfying $R_0 < 1$. Then, we separated the parameter values that give biphasic behavior from those that give triphasic behavior (see figure 6.1 for an example).

The model has twelve parameters. This number makes it very difficult to study their impact on the solution. Therefore we reduced the dimension of the parameter space to make the study feasable. Previous studies by Nowak *et al.* [35], Lewin *et al.* [44], Dahari *et al.* [41] and Ciupe *et al.* [42] explained what parameters can be fixed based on literature information. The parameters that mostly influence the transition between biphasic and triphasic patterns are (r_T, r_I, δ, ϵ). We vary these and fixed the rest to values obtained from the literature (see table 6.1 for details).

Next, we investigated the ranges for (r_T, r_I, δ, ϵ) that are needed for virus extinction, meaning, for the system to be stable at the free-disease state. This is given analytically by equation (5.9).

We start with the following ranges for the four parameters:

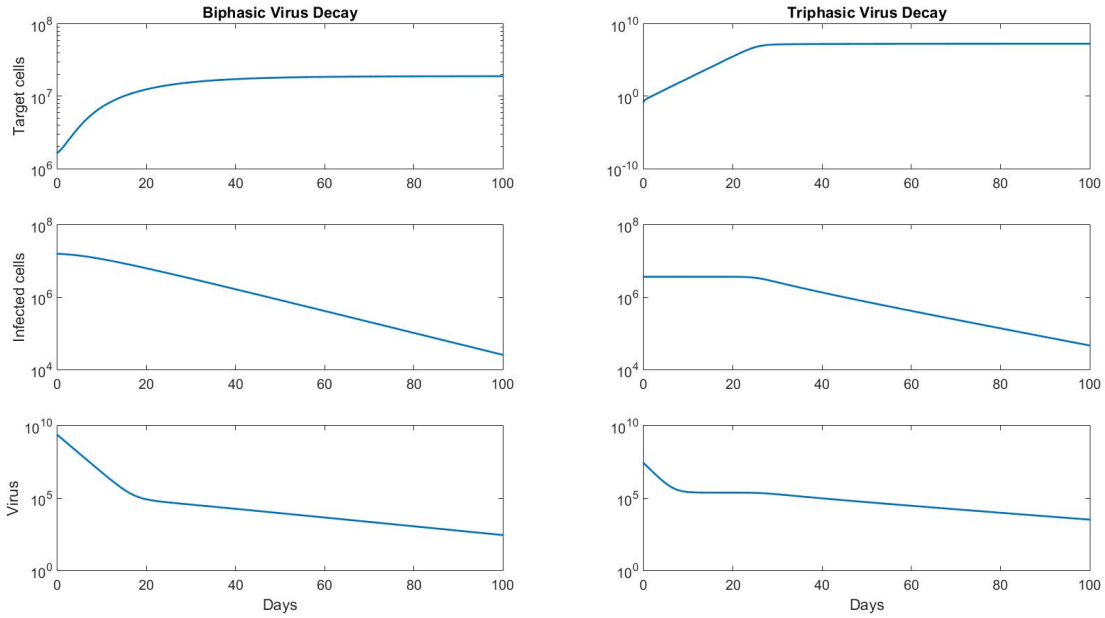

Figure 6.1: This two examples, with choice of parameters from [41], show the evolution of the three populations with time when decay of virus is biphasic (left) and when the decay is triphasic (right).

Parameter	Description	Value	Reference
s	production rate of T	1 cell/d/mL	[41]
d_T	death rate of T	0.01 /d	
β	rate of infection	10^{-10} mL/virions/d	[42]
K	natural level of target cells	1.9×10^7 cells/mL	[41]
ρ	recovery rate of I	0 /d	[41]
p	virus production	100 virions/cell/d	[43]
c	virus clearance	0.67 /d	[35]
η	effectiveness of therapy in blocking infection	0.5	[44]

Table 6.1: Fixed values of the parameters.

$$\begin{aligned} 0.2 < r_I, r_T < 4, \\ 0.01 < \delta < 0.1, \\ 0.7 < \epsilon < 1. \end{aligned} \tag{6.1}$$

This means that healthy and infected cell populations produce on average between 0.2 and

4 offsprings per day; the infected cells half life ranges between 7 and 69 days; and the drug is at least 70% efficacious. We use this as a starting point to create biphasic and triphasic patterns. This ranges were chosen by inspection of virus decay for several samples. Outside of these ranges, the virus clearance might not be observed either because $R_0 \geq 1$ and so there is no clearance at any time, or because clearance takes a long time to happen; and we do not want therapy to last more than one year.

6.1 Biphasic vs. Triphasic

The next step was to create a large number of samples, solve the system for each set, and separate the result into biphasic and triphasic. The fixed parameter values are as in table 6.1. The varying parameters are the production of target and infected cells, killing rate of infected cells and the effectiveness of therapy in blocking virion production with ranges given by (6.1).

Now we would like to know what parameter regions give rise to biphasic and triphasic. This may help optimize the therapy. The patient does not need to go through treatment during the flat phase since the drugs will not help with virus clearance. Knowing how long this phase lasts gives us an estimate on how long the patient can rest from treatment. A first intuition is that triphasic cases are "worst" since we have a phase in which the patient situation does not improve under therapy. We will discuss later how this factors in, but some triphasic cases are better than biphasic.

One of the challenges at this stage, was finding a clear definition of triphasic behavior; when do we say that we have an intermediate flat phase. Part of the code we used determines when the virus presents a flat phase and how long it lasts.

6.1.1 Determining phase behavior

Recall that our system has the form

$$\frac{d\vec{x}}{dt} = f(\vec{x}, \theta, t)$$

where $\vec{x} = (T, I, V)$ is the time-dependent state variable, $\theta = (r_T, r_I, \delta, \epsilon)$ are the varying parameters, and

$$f(\vec{x}, \theta, t) = \begin{pmatrix} s + r_T T\left(1 - \frac{T+I}{K}\right) - \beta V T - d_T T + \rho I \\ r_I I\left(1 - \frac{T+I}{K}\right) + \beta V T - (\delta + \rho) I \\ pI - cV \end{pmatrix}.$$

where $\{s, d_T, \beta, K, \rho, p, c, \eta\}$ are fix parameters with values as in table 6.1.

For each $\{r_T, r_I, \delta, \epsilon\}$ sample, we generate solutions of (5.1)-(5.3) that give the biphasic and triphasic patterns seen in patient data. Below we present the formal definition of biphasic and triphasic behavior for a solution $V(t)$ of (5.1)-(5.3). We choose parameter samples for which $R_0 < 1$.

Definition. We say that a solution $V(t)$ of (5.1)-(5.3) has *biphasic* behavior if

$$\frac{dV}{dt} < 0$$

for all $t > 0$.

Definition. We say that there is a *flat phase* when a solution $V(t)$ of (5.1)-(5.3) satisfies

$$\frac{dV}{dt} = 0$$

for some $t_1 \leq t \leq t_2$.

Definition. We say that a solution V of (5.1)-(5.3) has *triphasic* behavior when it presents a flat phase, i.e.,

$$\frac{dV}{dt} < 0, \qquad 0 < t < t_1,$$

$$\frac{dV}{dt} = 0, \qquad t_1 < t < t_2,$$

$$\frac{dV}{dt} < 0, \qquad t_2 < t.$$

We start with 8×10^6 different $\{r_T, r_I, \delta, \epsilon\}$ data sets generated randomly between boundaries (6.1). We solve the system and keep the samples with $R_0 < 1$, $0 < T < K$, $0 < I < K$, and $0 < V < 10^{10}$. We applied these definitions to separate our random generated samples between biphasic and triphasic. In the graphs shown in this chapter, we represent biphasic samples in black and triphasic samples in blue. Furthermore, for triphasic samples, we have different shades of blue that correspond with the length of the flat phase; the darker the blue point is the longer the flat phase is for that sample.

We obtained 230,083 triphasic samples and 788133 biphasic samples some of which are shown in figure 6.2. We found that biphasic behavior occurs more often than triphasic behavior. There is a clear difference between the region that defines biphasic behavior and the region that gives triphasic behavior. The region for triphasic seems to form an envelope around the region for biphasic. We found the projections of this 3D plot onto the planes and observed that the ratio r_T/r_I was an important factor for the behavior of the model, rather than the individual r_T and r_I values.

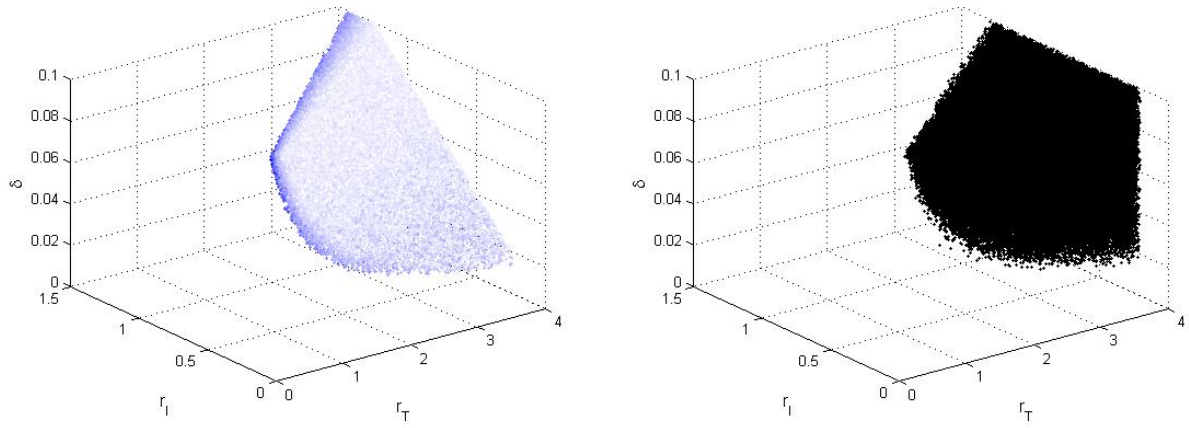

Figure 6.2: (r_T, r_I, δ) parameters that give triphasic (left) and biphasic (right) virus decay.

We then generated samples with: free $\delta \in [0.01, 0.1]$, free $\epsilon \in [0.7, 1]$, and fixed r_T/r_I; free $r_T/r_I \in [0.05, 20]$, free $\epsilon \in [0.7, 1]$, and fixed δ; free $r_T/r_I \in [0.05, 20]$, free $\delta \in [0.01, 0.1]$, and fixed ϵ. Results are shown in figure 6.3, 6.4, 6.5, respectively. These graphs show the relationship between $\delta - \epsilon$, $r_T/r_I - \epsilon$ and $r_T/r_I - \delta$ as well as the biphasic-triphasic regions. The samples accepted had $R_0 < 1$ and initial conditions $[T_0, I_0, V_0]$ such that

$$1e5 < T_0 < 1.9e7$$

$$0 < I_0 < 1.9e7$$

$$0 < V_0 < 1e10.$$

Note that the initial conditions have changed to make sure we start with enough healthy hepatocytes.

In figures 6.3, 6.4, 6.5, we can clearly see the difference between the triphasic region and the biphasic region. Also note that at the shared boundary of the regions, the triphasic samples have very short flat phase, i.e., they are close to be biphasic. For the three cases, all rejected samples satisfy the restriction on the initial condition but not $R_0 < 1$. This means that samples are rejected because the corresponding model will not show clearance of the virus.

Fixed $r_T/r_I = 5$.
In figure 6.3, we observe that our code rejected samples with $\delta < 0.055$. Therefore, in order for the free-disease steady state to be stable we need $\delta > 0.055$. We see that the region that guarantees stability is clearly divided into two regions: blue (triphasic) and black (biphasic). We have triphasic viral decay only if $0.05 < \delta < 0.065$ although for ϵ close to 1 ($\epsilon > 0.95$) most samples in such δ-interval are already biphasic. Also, for $\delta > 0.065$ we only obtain samples corresponding to biphasic decay of the virus. Biologically, this means that low killing of infected cells ($\delta < 0.055$) leads to virus persistence, independently of drug efficacy. This

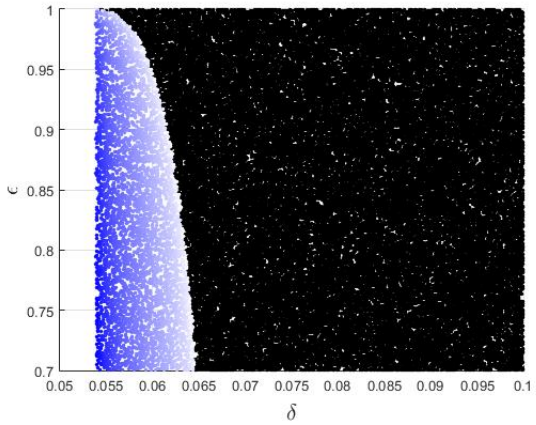

Figure 6.3: Biphasic vs. Triphasic with $r_T/r_I = 5$

is, therapy will not be successful if the immune response is weak. On the other hand, high killing of infected cells ($\delta > 0.065$), i.e., strong immune response guarantees biphasic decay of the virus. For intermediate killing rates of infected cells ($0.055 < \delta < 0.065$) high drug efficacy ($\epsilon > 0.98$) will give biphasic virus decay whereas triphasic decay is predicted for low drug efficacy ($\epsilon < 0.8$).

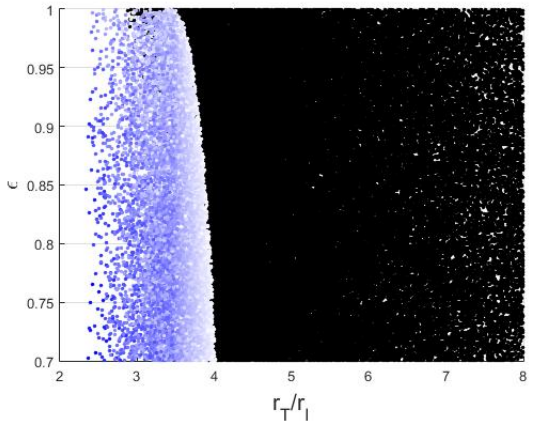

Figure 6.4: Biphasic vs. Triphasic with fix $\delta = 0.08$

Fixed δ.
In figure 6.4 we see a similar picture to the one in figure 6.3. First, samples for which the ratio is less than 2-2.5 are rejected because $R_0 < 1$. This means that virus will not clear if the proliferation of target cells is not, at least, double the proliferation of infected cells. We observe triphasic if $2.5 < r_T/r_I < 4$ and biphasic if $r_T/r_I > 4$. If drug efficacy is high enough, $\epsilon > 0.95$, we observe some overlap since we can get biphasic samples for

$2.5 < r_T/r_I < 4$. Biologically, if healthy hepatocytes do not proliferate at least twice as fast as infected hepatocytes, then the disease will persist no matter how efficacious the drugs are. But if healthy hepatocytes' growth rate is higher (more than quadruple) than the infected hepatocytes' growth rate, then the model predicts virus clearance in a biphasic manner.

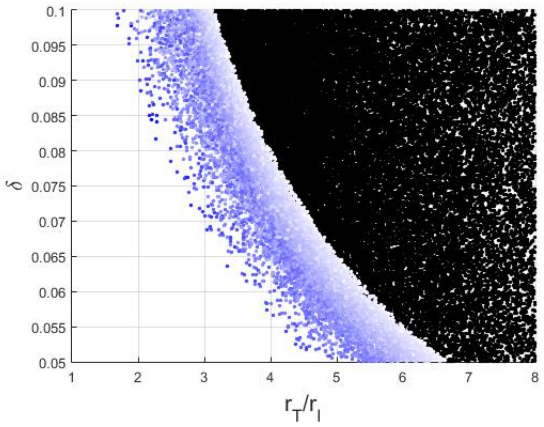

Figure 6.5: Biphasic vs. Triphasic with fix $\epsilon = 0.7$

Fixed ϵ.
The relation between r_T/r_I and δ is not as simple as the relation $\epsilon - \delta$ or $\epsilon - r_T/r_I$; the regions are not defined by vertical bands anymore. We can say that samples are rejected for $r_T/r_I \lesssim 2$ whereas the samples give biphasic virus decay if $r_T/r_I \gtrsim 6.5$. In the in-between region we find the "decaying triphasic band", of width approximately 1.5-2, that separates a lower region of rejected samples from an upper region of biphasic samples. Biologically, we see again that, to overcome the disease, the growth rate of hepatocytes needs to be at least twice higher than the growth rate of infected hepatocytes and immune response cannot be weak. Then our prediction gradually changes from triphasic to biphasic decays based on whether both the ratio between healthy and unhealthy hepatocyte production and the hepatocyte killing increase.

The summary of the information shown in figures 6.3, 6.4, 6.5, is that the domain of parameter values is split in three regions: low parameter values give no virus clearance; there is an intermediate band that give triphasic behavior; and high parameter values give biphasic behavior. Our results suggest that the effectiveness ϵ in blocking virion production does not play an important role on determining the outcome of our model; as long as drug efficacy is "reasonably" good enough ($\epsilon > 0.7$) all behaviors might be observed. We will see in the next section how high drug efficacy is necessary for *fast* virus clearance. We observed that δ and r_T/r_I cannot be both low or else virus clearance will not occur, i.e., we need a strong immune response to kill infected cells. We noted that the ratio r_T/r_I is always greater than one; this means that the healthy cells need to proliferate faster than the infected ones. While the killing rate can take a large range of values for the biphasic case, its values are high for low

proliferation ratio in the triphasic case. The high killing rate is in the patient's disadvantage. However high proliferation ratio compensates for it and helps liver regenerate.

6.2 Clearance time

Now that we know the difference between biphasic and triphasic in terms of the parameters, we want to know what parameters give a "good" behavior from a biological point of view. So far we have only asked for viral decrease. Now, we do not want a patient to be on drugs for longer than a year, so we want the virus to be cleared fast (in less than a year). This is why the next step on our study is finding out what parameter values give a short clearance time. To do so, we generated parameter samples in the same ranges but with two fix parameters and used an ODE solver to record the value of the virus at each time from 0 to 2000. We then checked the first time for which $V \leq 3 \times 10^{-4} = 1$ virion per mL and consider that is the time at which we have clearance of the virus, since we assume the virus distributes through 3L of blood.

We generated samples with: free $r_T/r_I \in [0.05, 20]$ and fix δ, ϵ; free $\delta \in [0.01, 0.1]$ and fix $r_T/r_I, \epsilon$; free $\epsilon \in [0.7, 1]$ and fix $r_T/r_I, \delta$. Since a lot of samples were rejected, we changed the acceptance condition of the initial values $[T_0, I_0, V_0]$ to

$$0.2K < T_0 + I_0 < K$$

$$0 < T_0 < 1.9e7$$

$$0 < I_0 < 1.9e7$$

$$0 < V_0 < 1e10.$$

Biologically, this condition means that we accept the samples for which the liver has enough cells to fully regenerate and overcome the disease.

In figures 6.6, 6.7, 6.8 we include some of the resulting figures showing the relation between parameter values and virus clearance time. The "good" samples are the ones for which the virus is cleared in less than one year.

Note on figure 6.6: The graphs present very light blue points following the triphasic samples. These points are far from the biphasic part of the graph. This seems to contradict our analysis: the lighter the blue the closer to biphasic behavior. Based on inspection of such samples, we hypothesize that the virus decay for these samples presents another flat phase. Since more work needs to be done to analyze these samples, we will not include them in the following discussion.

Clearance vs. r_T/r_I.
We see in figure 6.6 that again the ratio r_T/r_I must be greater than one to obtain good results. We observe, in general, biphasic samples clear faster than triphasic samples. In

any case, the higher the ratio is, the faster the clearance occurs. Note that the samples shown have drug efficacy 0.9 or 0.95 and killing rate of infected cells 0.06 or 0.08 per day. However, in neither case, not even when production of hepatocytes is 8 times faster than the production of infected cells, we predict virus clearance in less than a year. The following analysis of the figures 6.7 and 6.8 will clarify what is needed for fast clearance.

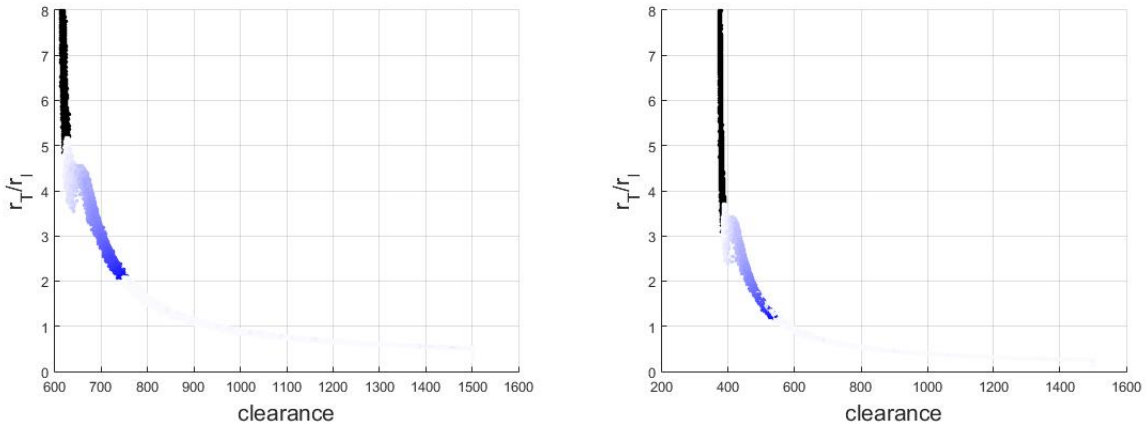

Figure 6.6: Clearance time vs. r_T/r_I

Left: $\delta = 0.06$, $\epsilon = 0.9$. Right: $\delta = 0.08$, $\epsilon = 0.95$.

Clearance vs. δ.
The description of the relationship clearance-δ is similar to the one for clearance-ratio made above in that the larger the parameter value is, the fater the virus clears. In this case we do observe samples for which the virus is expected to clear in less than a year of therapy. For such outcome, we need a high rate of killing of infected cells ($\delta > 0.095$). Therefore, as we suggested earlier, drugs alone are not sufficient and a strong immune response is beneficial. This is corroborated by our next analysis (figure 6.8).

Clearance vs. ϵ.
Figure 6.8 agrees with the natural asumption that the more efficacious treatment is, the faster clearance we obtain. Note that if $\delta = 0.05$, clearance occurs when ϵ is almost 1 (at least 0.9999). That means that a weak immune response would require treatment to be almost 100% efficient in blocking virion production in order to get virus clearance. The right graph in figure 6.8 shows that if there is strong immune response ($\delta > 0.07$) and if target cells production is higher than infected cells production ($r_T/r_I > 5$) then therapy with "reasonable" efficacy ($\epsilon > 0.95$) will give a good outcome.

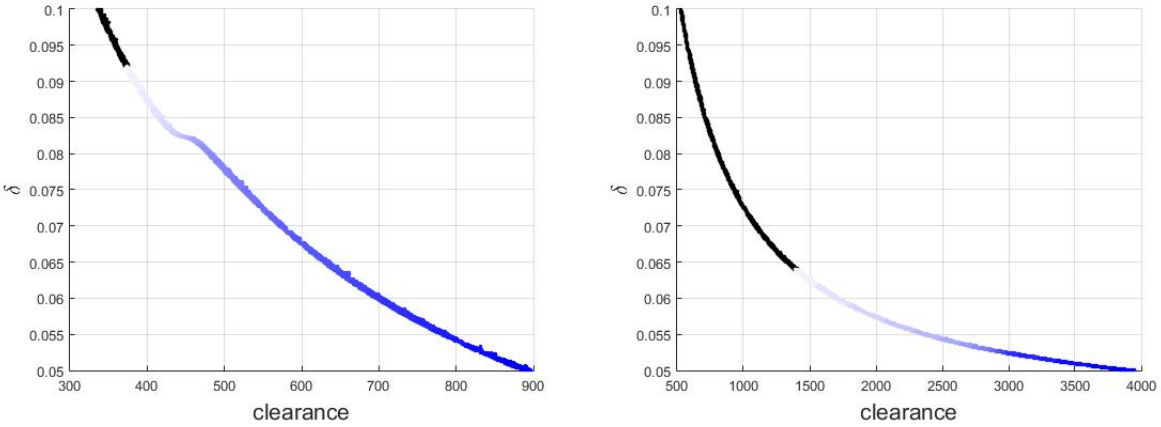

Figure 6.7: Clearance time vs. δ

Left: $r_T/r_I = 3$, $\epsilon = 0.9$. Right: $r_T/r_I = 5$, $\epsilon = 0.7$.

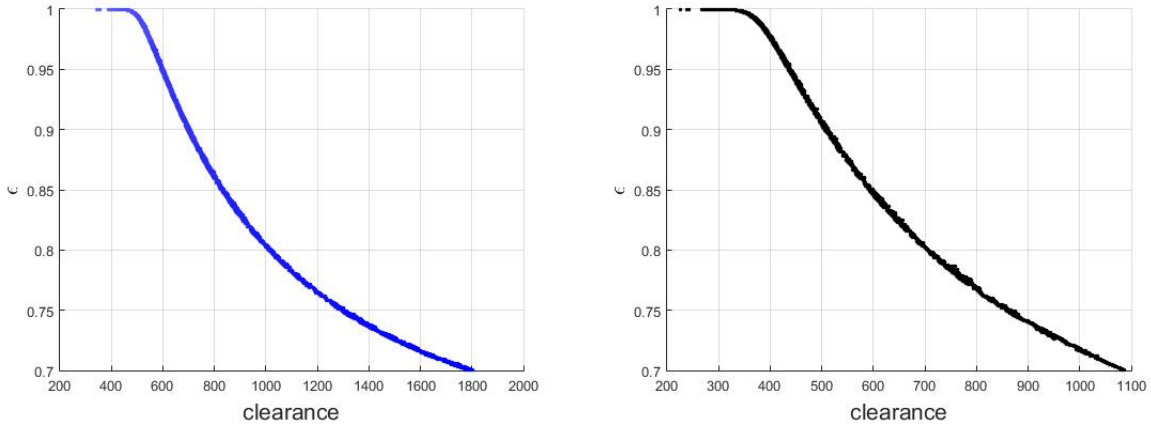

Figure 6.8: Clearance time vs. ϵ

Left: $r_T/r_I = 3$, $\delta = 0.06$. Right: $r_T/r_I = 6$, $\delta = 0.07$.

6.3 Liver damage

As mentioned earlier, during drug therapy the immune response is active as well. While HBV does not itself lead to liver loss, the hepatocytes die due to cytopathic immune responses [5]. The liver has the ability to regenerate [53]. If at any moment the liver is reduced to less than 25% then the patient dies [22]. For every sample we have used in this chapter, we checked the amount of liver cells at each time of treatment with the condition $T + I <$

$0.2 \times 13.6 \times 10^6 = 2.72 \times 10^6$. The results were positive for all cases; all samples predict that the subject would survive since they would never lose more than 20% of their liver at any point throughout therapy.

6.4 Discussion

Dahari *et al.* provide a model (5.1)-(5.3) that explains complex virus decay of HBV patients undergoing therapy. Here we extend their analytical analysis and investigated the parameter space that gave rise to the observed patterns of decay.

From the analytical analysis, we have the R_0 condition that differentiates virus decay from virus rebound or virus with final flat phase. We have focused our numerical analysis on differentiating biphasic from triphasic decay. The figures in this section suggest that the parameter values that predict biphasic decay of the virus is separated from the region that predicts triphasic behavior.

In terms of clearance time, we found that strong immune response is needed for virus to decay below limit of detection in less than a year. Moreover, production rate of healthy hepatocytes has to be at least double the production of infected hepatocytes. In general, the figures show that the shortest clearance time corresponds to the biphasic samples. Therefore, if we could define the parameter region that gives biphasic behavior then we have the region that predicts the best outcomes.

Chapter 7

Final notes

Hepatitis B is a dangerous disease that affects people all over the world and causes millions of deaths every year. There exists a successful vaccine, but it is not available worldwide so its effects in eradicating the virus will take some years. Until then, we need to improve the therapies available for infected patients. There are seven approved drugs for the treatment of patients with Hepatitis B. Several studies explain the effects of these drugs and shed some light on how treatment should proceed depending on each patients characteristics. Over the years, mathematical models and their analysis have helped understand the biological interactions behind hepatitis B infection, persistence or clearance following therapy. One of the unanswered questions regards the relationship between the pattern of virus decay and the success of the treatment. Dahari *et al.* developed a model that can predict the different viral decay patterns: biphasic decay, triphasic decay, stepwise decay, flat second phase, and rebound. The outcome of the model depends on the value of twelve parameters. In this thesis we have focused on analyzing this model and determining how the parameter values could affect the strategy for treatment.

Our analytical results give a condition to separate the possible viral decay profile into two groups: virus persistence and virus clearance. If R_0 in (5.9) is bigger than 1 then the decay profile is either rebound or second flat phase. If R_0 is less than 1 then the decay profile is biphasic, triphasic, or stepwise decay. This condition can be rewritten in terms of drug efficacy, with $\epsilon_{tot} > \epsilon_c$ implying viral clearance and $\epsilon_{tot} \leq \epsilon_c$ implying viral rebound. Our predictions match when referring to biphasic decay, triphasic decay, virus rebound, and second flat phase. In this study, we focus then on finding the difference between biphasic and triphasic decay. Future work may include differentiating these from stepwise decay.

When numerically investigating the model, we determined that, although twelve parameters affect the model solution, only four of them seem to determine the differences in decay profiles. These parameters are the drug efficacy ϵ in blocking virion production, the killing rate δ of infected cells, and the ratio r_T/r_I of growth rate of healthy and infected hepatocytes. Numerical results showed that the parameter space where the disease free equilibrium is

stable, is divided between samples with biphasic and triphasic viral decay. We have also shown that the region in the parameter space that gives fast virus clearance is a subset of the region that gives biphasic decay.

We were able to confirm what other papers had suggested related with treatment success [41]. If the treatment is almost 100% effective in blocking virion production then, as long as the disease-free steady state is stable, we will get biphasic decay and fast clearance of the virus. If we relax our condition on drug effectiveness to a more reasonable level of 90%, then we predict that strong immune response is needed for clearance. Moreover, the production of healthy hepatocytes must at least double the production of infected cells. Our numerical results have given us a clear definition of the parameter ranges that predict good outcome, when several parameter values stay fix.

In summary, we have investigated a model of hepatitis B dynamics under drug therapy. Using analytical techniques we determined when the virus will be cleared or persist. Using numerical techniques, we predicted the types of viral decay. Our results provide a framework for the virological and immunological factors involved in a successful drug therapy. Such knowledge can inform drug design.

Bibliography

[1] Z Sandor, P Andras. Alternative sampling methods for estimating multivariate normal probabilities. *Econometric Institute Report EI*, 2003,05.

[2] N Bacaër. *Daniel Berboulli, d'Alembert and the inoculation of smallpox (1760). In* A Short History of Mathematical Population Dynamics *(p. 21-30).* Springer London, 2011.

[3] WL Oberkampf, MF Barone. Measures of agreeement between computation and experiment: validation metrics. *J og comput. Phys.*, 217:5–36, 2006.

[4] D Bernoulli. Essai d'unne nouvelle analyse de la mortalité causée par la petite vérole. *Mem Math Phys Acad Roy Sci*, 1, 1766.

[5] LG Guidotti, FV Chisari. Immunobiology and pathogenesis of viral hepatitis. *Annu Rev Pathol*, 1:23–61, 2006.

[6] LG Guidotti, R Rochford, J Chung, M Shapiro, R Purcell, FV Chisari. Viral clearance without destruction of infected cells during acute HBV infection. *Science*, 284:825–829, 1999.

[7] LG Guidotti, T Ishikawa, MV Hobbs, B Matzke, R Schreiber, FV Chisari. Intracellular inactivation of the hepatitis B virus by cytotoxic T lymphocytes. *Immunity*, 4(1):25–36, 1996.

[8] P Lampertico, A Aghemo, M Vigano, M Colombo. HBV and HCV therapy. *Virusses*, 1:484–509, 2009.

[9] S Zeuzem, RA de MAn, P Honkoop, WK Roth, SW Schalm, JM Schmidt. Dynamics of hepatitis B virus infection in vivo. *J Hepatol*, 27:431–436, 1997.

[10] R Ghanem, A Doostan. On the construction and analysis os stochastic models: characterization and propagation of the errors associated with limited data. *J of comput. Phys.*, 217:6381, 2006.

[11] SM Blower, H Dowlatabadi. Sensitivity and uncertainty analysis of complex models of disease transmission: an HIV model, as an example. *Int Stat Rev*, 62(2):229–43, 1994.

[12] S Kirmizialtin, KA Johnson, R Elber. Enzyme selectivity of HIV reverse transcriptase: Conformations, ligands, and free energy partition. *J Phys Chem B*, 119(35):11513–11526, 2015.

[13] ND Theise, R Saxena, BC Portmann, SN Thung, H Yee, *et al.* The canals of hering and hepatic stem cells in humans. *Hepatology*, 30:1425–1433, 1999.

[14] A Perelson, P Essunger, Y Cao, M Vesanen, A Hurley, K Saksela, M Markowits, et al. Decay characteristics of hiv-1-infected compartments during combination therapy. *NAture*, 387:188–191, 1997.

[15] P Colombatto, L Civitano, R Bizzarri, F Oliveri, S Choudhury, R Gietschke, et al. A multiphase model of the dynamics of HBV infection in HBeAg-negative patients during pegylated interferon-alpha2a, lamivudine and combination therapy. *Antivir Ther*, 11:197–212, 2006.

[16] X Wei, SK Ghosh, ME Taylor, VA Johnson, EA Emini, P Deutsch, JD Lifson, et al. Viral dynamics in human immunodeficiency virus type 1 infection. *Nature*, 373:117–122, 1995.

[17] O Nissim, M Melis, G Diaz, DE Kleiner, A Tice, G FAntola, F Zamboni, L Mishra, P Farci. Liver regeneration signature in hepatitis B virus (hbv)-associated acute liver failure identified by gene expression profiling. *PLoS*, 7(11), 2012.

[18] KJ Riehle, YY Dan, JS Campbell, N Fausto. New concepts in liver regeneration. *J Gastroenterol Hepatol*, 26:203–212, 2011.

[19] A Ponzetto, PJ Cote, EC Ford, RH Purcell, JL Gerin. Core antigen and antibody in woodchucks after infection with woodchuck hepatitis virus. *J. Virol.*, 52:70–76, 1984.

[20] BC Tennant, JL Gerin. The woodchuck model of hepatitis b virus infection. *ILAR J*, 42(2):89–102, 2001.

[21] M Tsiang, JF Rooney, JJ Toole, CS Gibbs. Biphasic clearance kinetics of hepatitis B virus from patients during adefovir dipivoxil therapy. *Hepatology*, 29(2):1863–1869, 1999.

[22] D Häussinger. *Liver regeneration.* De Gruyter, Berlin, 2011.

[23] World Health Organization. *Guidelines for the prevention, care and treatment of persons with chronic hepatitis B infection.* WHO Library Cataloguing-in-Publication Data, 2015.

[24] M Pilch, TG Trucano, JC Helton. Ideas underlying quatification of margins and uncertainties (QMU) : a white paper. *Sandia report*, 2006.

[25] WL Oberkampf, JC Helton. Investigation of evidence theory for engineering applications. *AIAA Non-deterministic approaches forum, Denver, Colorado*, pages 2002–1569, 2002.

[26] AS Perelson, AU Neumann, M Markowitz, JM Leonard, DD Ho. Hiv-1 dynamics in vivo: virion clearance rate, infected cell life-span, and viral generation time. *Science*, 271(5255):1582–1586, 1996.

[27] B Su, W Shou, KS Dorman, DE Jones. Mathematical modelling of immune response in tissues. *Comp and Math methods in Med*, 10(1):9–38, 2009.

[28] DJ Covert, D Kirschner. Revisiting early models of the host-pathogen interactions in HIV infection. *Comments Theor Biol*, 5(6):383–411, 2000.

[29] D Lavanchy. Hepatitis B virus epidemiology, disease burden, treatment, and current and emerging prevention and control measures. *J Viral Hepat*, 11(2):97–107, 2004.

[30] AS Lok. Personalized treatment of hepatitis B. *Clin Mol Hepatol*, 21(1):1–6, 2015.

[31] C Trepo, HLY Chan, A Lok. Hepatitis b virus infection. *Lancet*, 384(9959):2053–2063, 2014.

[32] D Ho, A Neumann, A Perelson, W Chen, J Leonard, M Markowitz. Rapid turnover of plasma virions and cd4 lymphocytes in hiv-1 infection. *NAture*, 373:123–126, 1995.

[33] C Seeger, WS Mason. Hepatitis B Virus Biology. *Microbiol Mol Biol Rev*, 64(1):51–68, 2000.

[34] K Kajino, AR Jilbert, J Saputellu, CE Aldrich, J Cullen, WS Mason. Woodchuck hepatitis virus infections: very rapid recovery after a prolonged viremia and infection of virtually every hepatocyte. *J. Virol.*, 68:5792–5803, 1994.

[35] MA Nowak, S Bonhoeffer, AM Hill, R Boehme, HC Thomas, H McDade. Viral dynamics in hepatitis B virus infection. *Proc. Natl. Acad. Sci. USA*, 93:4398–4402, 1996.

[36] AS Lok, BJ McMahon. Chronic hepatitis B: Update of recommendations. *Hepatology*, 39(3):857–861, 2004.

[37] American Institute of Aeronautics and Astronautics. *Guide for the verification and validation of computational fluid dynamics simulations*. AIAA-G-077-1998, Reston, VA.

[38] AS Perelson. Modelling viral and immune system dynamics. *Nature Reviews Immunology*, 2:28–36, 2002.

[39] AU Neumann, NP Lam, H Dahari, DR Gretch, TE Wiley, TJ Layden, AS Perelson. Hepatitis C viral dynamics in vivo and the antiviral efficacy of interferon-alpha therapy. *Science*, 282:103–107, 1998.

[40] GQ Witten, AS Perelson. Modeling the cellular-level interaction between the immune system and hiv. *South African Journal of Science*, 100:1–5, 2004.

[41] H Dahari, E Shudo, RM Ribeiro, AS Perelson. Modeling complex decay profiles of Hepatitis B virus during antiviral therapy. *Hepatology*, 1:49:32–38, 2009.

[42] SM Ciupe, RM Ribeiro, PW Nelson, AS Perelson,. Modeling the mechanisms of acute hepatitis B virus infection. *J Theor Biol.*, 247(1):23–35, 2007.

[43] SM Ciupe, RM Ribeiro, PW Nelson, G Dusheiko, AS Perelson,. The role of cells refractory to productive infection in acute hepatitis B viral dynamics. *PNAS*, 104(12):5050–5055, 2007.

[44] SR Lewin, RM Ribeiro, T Walters, GK Lau, S Bowden, S Locarnini, AS Perelson. Analysis of hepatitis B viral load decline under potent therapy: complex decay profiles observed. *Hepatology*, 34(5):1012–1020, 2001.

[45] LF Barker, FV Chisari, PP McGrath, DW Dalgard, RL Kirschstein, LD Almeida, TS Edington, DG Sharp, MR Peterson. Transmission of type B viral hepatitis to chimpanzees. *J Infect Dis*, 127(6):648–62, 1973.

[46] TG Trucano, LP Swiler, T Igusa, WL Oberkampf, M Pilch. Calibration, validation, and sensitivity analysis: What's what. *Reliability engineering and system safety*, 91:1331–1357, 2006.

[47] J. A. Rice. *Mathematical statistics and data analysis*. Duxbury Press, 1995.

[48] N Fausto, JS Campbell, KJ Riehle. Liver regeneration. *Hepatology*, pages 45–53, 2006.

[49] A Bertoletti, L Rivino. Hepatitis B: future curative strategies. *Curr Opin Infect Dis*, 27(6):528–534, 2014.

[50] J-T Guo, H Zhou, C Liu, C Aldrich, J Saputelli, T Whitaker, MI Barrasa, WS Mason, C Seeger. Apoptosis and regeneration of hepatocytes during recovery from transcient hepadnavirus infections. *Journal of Virology*, 74(3):1495–1505, 2000.

[51] S Fersin, RB Nel sen, *et al.* Dependence in probabilistic modeling, Dempster-Shafer theory, and probability bounds analysis. *SAND Report*, page 3072, 2004.

[52] SL Butler, G Sinha. Forward modeling of applied geophysics methods using Comsol and comparison with analytical and laboratory analog models. *Computers and Geosciences*, 42:168–176, 2012.

[53] DH van Thiel, JS Gavaler, I Kam, A Francavilla, L Polimeno, RR Schade, J Smith, W Diven, RJ Penkrot, TE Starzl. Rapid growth of an intact human liver transplanted into a recipient larger than the donor. *Gastroenterology*, 93:1414–1419, 1987.